Molecular Structure of Carbene Analogues: A Computational Study

Ágnes Szabados and Magdolna Hargittai*

Structural Chemistry Research Group of the Hungarian Academy of Sciences, P.O. Box 32, Eötvös University, H-1518 Budapest, Hungary

Received: November 15, 2002; In Final Form: March 6, 2003

Systematic computational studies on the dihydrides and dihalides of group 14 elements have been performed, for their ground state and first excited state. We present equilibrium geometries of the lowest lying singlet and triplet states and singlet−triplet energy separation data on the whole series obtained by the CCSD(T) method. Scalar relativistic effects are taken into account by applying effective core potentials (ECP) from the fourth period on. The performance of two sets of core potentials is compared and set against previous theoretical results and available experimental information. Expected trends and anomalies in the variation of geometrical parameters are discussed.

I. Introduction

In a recent review of the molecular structure of carbene analogues[1] we found certain discrepancies between the available experimental and computational data, as well as between different computational results. To have a clearer picture on the regularities in the structures of these relatively simple molecules, we decided to carry out a systematic computational study of all molecules involved at a high and consistent computational level.

The structure and properties of carbene and its analogues have been the subject of numerous previous investigations. Especially methylene[2−4] and its halogen derivatives[5−13] have received much interest recently by computations, whereas relatively fewer studies appeared on the heavier analogues (i.e., substituting carbon by other members of its group).[14−18]

Focusing mainly on relativistic effects, Balasubramanian and co-workers performed systematic studies on AX_2 molecules, A = Ge, Sn, Pb, X = H, F, Cl, Br, I, during the 1990s.[14−17] They carried out multireference configuration interaction calculations including single and double excitations (MRSDCI), with the complete active space self-consistent field (CASSCF) wave function as the reference function. Besides the ground state, they characterized several excited states as well. Scalar relativistic effects were accounted for in their studies by applying the relativistic effective core potentials of Christiansen et al.,[19−22] furthermore, spin−orbit coupling was described in some of their works by explicit inclusion of a spin−orbit operator at a subsequent relativistic CI stage. Relativistic effects were found important for lead being the central atom, whereas the effect of relativity originating from a ligand of large atomic number, such as iodine, was not that striking.

The performance of density functional theory (DFT) was tested by Escalante et al.,[18] addressing the $^1A_1$ state of AX_2 and AX_4 molecules (A = C, Si, Ge, Sn, Pb and X = F, Cl, Br, I). They considered three different exchange correlation functionals together with the ECPs of the Stuttgart/Bonn group.[23] Interestingly, they found that equilibrium geometries calculated by the Hartree−Fock (HF) method were as good as their best DFT results (using an exchange-correlation functional based on the local spin density approximation). Both nonrelativistic and quasi-relativistic ECPs were applied in their study, so that scalar relativistic effects could be analyzed in detail. When geometries produced by the two ECPs were compared, bond contraction of bromides and iodides and an increase in the bond angle of lead dihalides were the most noticeable effects found.

The most recent theoretical studies addressing only methylene and/or its halogen derivatives include that of Garcıa et al.,[5] Das and Whittenburg,[6] Schwartz and Marshall,[7] and Sendt and Bacskay.[8] The experimental singlet−triplet gap of CCl_2 reported by Lineberger and co-workers[9] has initiated further investigations such as the one of Barden and Schaefer,[10] Lee et al.,[11] Hajgató et al.,[12] and Hargittai et al.[13]

The above works vary much in the sophistication of the theory and the dimension of the basis set. Thus, the large number of computational data of various accuracies on the different AX_2 molecules makes it hard to draw conclusions on the variation of structural parameters.[1] Of the two studies covering most of the molecules of this family, that of Escalante et al.[18] does not include data on the triplet states, whereas the works of Balasubramanian et al.[14−17] miss the compounds with C and Si being the central atom. The motivation of the present work was to produce a set of data on the lowest singlet and triplet states of the whole series favoring consistency of the calculations. Our goal with this study is to look at the variation of geometrical parameters from the structural chemistry point of view.

II. Computational Details

As single reference based approaches to count for electron correlation were found sufficient for a good description of the ground and the first excited states of these molecules,[7,8] we have carried out coupled cluster calculations including single and double excitations and counting for triples perturbatively (CCSD(T) and UCCSD(T) for the $^1A_1$ and the $^3B_1$ state, respectively). Full geometry optimizations were performed by the GAUSSIAN 98 program package,[24] using the frozen core approximation throughout. Cutoffs for determining a minimum on the potential energy surface were the default values of GAUSSIAN 98.

Though the coupled cluster method based on an unrestricted Hartree−Fock (UHF) determinant does not result in an ap-

* To whom correspondence should be addressed. E-mail: hargittaim@ludens.elte.hu.

10.1021/jp027466j CCC: $25.00
Published on Web 05/03/2003

TABLE 1: Computed Equilibrium Bond Lengths [r_e(A−X)/Å] for AX_2 Molecules in Their Ground and First Excited States (A = C, Si, Ge, Sn, Pb; X = H, F, Cl, Br, I)[a]

elec state	$^1A_1$					$^3B_1$				
	C	Si	Ge	Sn	Pb	C	Si	Ge	Sn	Pb
					CCSD(T)/EC[b]					
H	1.111	1.523	1.564	1.750	1.852	1.078	1.484	1.511	1.693	1.780
F	1.303	1.608	1.714	1.853	2.076	1.317	1.606	1.705	1.840	2.075
Cl	1.730	2.089	2.200	2.357	2.500	1.685	2.063	2.164	2.326	2.509
Br	1.894	2.249	2.397	2.552	2.659	1.840	2.223	2.369	2.530	2.693
I	2.094	2.470	2.633	2.786	2.867	2.020	2.436	2.604	2.765	2.909
					CCSD(T)/ST[c]					
H	1.111	1.523	1.600	1.784	1.847	1.078	1.484	1.544	1.725	1.773
F	1.303	1.608	1.750	1.934	2.046	1.317	1.606	1.741	1.924	2.057
Cl	1.730	2.089	2.205	2.380	2.494	1.685	2.063	2.178	2.357	2.519
Br	1.906	2.263	2.370	2.539	2.648	1.850	2.236	2.349	2.522	2.687
I	2.114	2.490	2.588	2.757	2.858	2.040	2.453	2.564	2.739	2.902

[a] CCSD(T) within the frozen core approximation; ECPs are applied on atoms Ge, Br, Sn, I and Pb. For other details see text. [b] Relativistic ECPs of Christiansen et al. [c] Relativistic ECPs of the Stuttgart/Bonn group.

propriate spin eigenfunction, the spin contamination of the $^3B_1$ state at the UHF level was rather small; therefore, we assumed that no serious error was introduced by this. This assumption was made in some of the earlier studies as well.[11,12]

In the first series of calculations (CCSD(T)/EC) the same or similar basis sets and effective core potentials were used as the ones in refs 14−17 (MRSDCI/EC), to see the difference produced by the different theoretical approaches, excluding effects coming from the basis set. Thus, from the fourth period on, the relativistic ECPs of Christiansen et al. were used,[20−22] both on the central atom and the ligand, retaining the outermost s^2p^2 and s^2p^5 shells, respectively. Valence basis sets for the central atoms were 4s4p1d, designed as follows. In the case of Ge and Sn we uncontracted the basis given in refs 20 and 21 and augmented them by an (s, p, d) diffuse set taken from ref 14. As for Pb, to the 4s4p set of ref 14 we added a diffuse d function with an exponent of 0.0801. The bases for the ligands were 3s2p sets also produced by uncontracting the basis of refs 20 and 21 and adding one d function for both Br and I, with the exponents being 0.338 and 0.302, respectively.[25,26] Dunning's cc-pVTZ basis sets were applied for the elements of the first three periods.[27,28]

There are still some differences between the ECPs and basis sets of the CCSD(T)/EC and MRSDCI/EC series (i.e., in MRSDCI/EC the outermost d^{10} shells were taken out of the ECPs of the central atom for the hydrides; ECPs were applied for F and Cl in MRSDCI/EC, whereas in our calculations we used all-electron bases for these atoms). Therefore, the difference in the two series of results, which essentially originates in the different theoretical approaches, may have been influenced somewhat by the differences in the ECPs and basis sets mentioned above.

In our second set of computations (CCSD(T)/ST), quasi-relativistic ECPs of the Stuttgart/Bonn group were applied, again from the fourth period on, retaining the same valence shells as before.[23] Of the corresponding basis sets[29] we used the valence polarized triple-ζ type sets, namely (14s10p2d1f)/[3s3p2d1f] for Ge, Br, Sn, and I,[30] and a (4s4p1d)/[2s2p1d] basis for Pb.[31] For AX_2 molecules where A = C, Si and X = H, F, Cl Dunning's cc-pVTZ basis sets were applied again. The CCSD(T)/EC and CCSD(T)/ST results are therefore identical for molecules consisting of atoms of the first three periods only.

Because our main goal with this work was to find trends in structural parameters along the series, it was essential that the basis sets be chosen right. This is not an obvious task considering that atoms of very different sizes are involved, starting from hydrogen up to lead and iodine. To make sure that the introduction of ECPs in the middle of the group does not bring in unwanted parameter changes, we tested its effect by altering the row of the periodic table at which we started to apply ECPs. First, geometries were reoptimized at the CCSD(T) level, introducing Stuttgart ECPs already at the third row. Next, we shifted the introduction of ECPs to the fifth row of the periodic table (i.e., all-electron basis sets were used for the fourth period elements) and again reoptimized the geometries at the CCSD(T) level. In both cases we were careful not to change the dimension of the basis and the number of electrons involved in the calculation of electron correlation. For this reason, the 2s2p basis set[23] corresponding to the Stuttgart ECP of Si was augmented by a d function with an exponent of 0.5342 (optimized at the HF level, for the SiH_2 molecule at experimental geometry), and by a further (s, p, d, f) diffuse set[28] from the EMSL basis set database.[32] In the case of chlorine we added two d functions (with exponents 1.046 and 3.444) and one f function (with exponent 0.706) to the basis set given with the Stuttgart ECP,[23] and uncontracted the last primitive Gaussian of the first s function of the Stuttgart basis. For the reverse check on the fourth period the ECPs of Ge and Br were changed to Dunning's cc-pVTZ basis set.[33]

For the lead derivatives we also checked the effect of a quasi-relativistic description of the atomic cores (using ECPs) on the equilibrium geometry compared to the nonrelativistic description. For this purpose we took the nonrelativistic ECP[31] of the Stuttgart/Bonn group on Pb and reoptimized the geometries of PbX_2 molecules, X = H, F, Cl, Br, I. The nonrelativistic basis set on Br was cc-pVTZ, whereas for iodine the (18s,12p,7d)/[6s,5p,3d] basis labeled "MIDI!" in the EMSL database[32] was uncontracted to a [7s6p3d] and augmented by an f function with exponent 0.2592. (The f exponent was optimized for the PbI_2 molecule at the HF level, at experimental geometry.)

Simple differences of total energies are reported as singlet−triplet gaps. We ignored zero point energy (ZPE) correction, because its effect is shown to be smaller than the basis set effects or the effects due to the different approximations of the different theoretical approaches;[12] consequently, the ZPE correction is not expected to alter the observed trends.

III. Results and Discussion

The computed geometrical parameters for all ground state and first excited state AX_2 molecules are given in Tables 1 and 2. For comparison, the experimentally determined bond lengths

TABLE 2: Computed Equilibrium Bond Angles [∠X−A−X/deg] for AX_2 Molecules in Their Ground and First Excited States (A = C, Si, Ge, Sn, Pb; X = H, F, Cl, Br, I)[a]

elec state	$^1A_1$					$^3B_1$				
	C	Si	Ge	Sn	Pb	C	Si	Ge	Sn	Pb
					CCSD(T)/EC[b]					
H	101.6	92.3	91.3	91.6	91.2	133.5	118.4	119.7	118.7	119.4
F	104.9	100.7	97.4	96.3	98.9	119.4	113.2	113.6	111.5	120.9
Cl	109.1	101.6	100.3	98.4	100.4	127.8	118.1	118.3	116.6	124.5
Br	110.8	103.0	102.2	100.2	101.9	129.9	119.8	120.7	120.0	128.1
I	113.1	104.5	103.7	101.5	102.7	133.9	121.8	123.1	122.8	129.0
					CCSD(T)/ST[c]					
H	101.6	92.3	91.2	91.4	90.9	133.5	118.4	119.3	118.9	120.6
F	104.9	100.7	97.8	96.4	97.0	119.4	113.2	113.3	112.7	121.7
Cl	109.1	101.6	100.1	98.4	98.9	127.8	118.1	118.7	117.3	126.3
Br	109.9	102.6	101.5	99.5	100.3	129.4	119.7	120.9	119.2	128.6
I	112.0	103.3	102.4	100.1	100.8	132.8	121.2	122.3	120.7	128.2

[a] CCSD(T) within the frozen core approximation; ECPs are applied on atoms Ge, Br, Sn, I, and Pb. For other details see text. [b] Relativistic ECPs of Christiansen et al. [c] Relativistic ECPs of the Stuttgart/Bonn group.

TABLE 3: Experimental Geometrical Parameters for $^1A_1$ States of AX_2 Molecules[a]

	C	Si	Ge	Sn	Pb
			r(A−X)/Å[b]		
H	1.107(2)[c]	1.5140[i]	1.591(7)[n]	-	-
F	1.3035(1)[d]	1.5901(1)[j]	1.7321(2)[o]		2.036(3)[t]
	1.300[e]				2.041(3)[x]
Cl	1.7157(28)[f]	2.088(4)[k]	2.186(4)[p]	2.345(3)[t]	2.447(5)[y]
	1.714(1)[g]	2.076(4)[l]	2.16945(2)[q]	2.338(3)[u]	2.444(5)[y]
		2.065310(26)[m]		2.335(3)[v]	
Br	1.74[h]	2.249(5)[k]	2.359(5)[r]	2.512(3)[w]	2.597(3)[z]
		2.227(6)[l]		2.504(3)[u]	
				2.501(3)[v]	
I	-	-	2.540(5)[s]	2.706(4)[w]	2.804(4)[t]
				2.699(3)[u]	
				2.688(6)[v]	
			∠(X−A−X)/deg		
H	102.4(4)[c]	92.08[i]	91.2(8)[n]	-	-
F	104.78(2)[d]	100.76(2)[j]	97.148(30)[o]	-	96.2(22)[t]
	104.94[e]				
Cl	109.2(3)[f]	102.8(6)[k]	100.3(4)[p]	98.5(20)[t]	98.7(10)[y]
	109.3(1)[g]	104.2(6)[l]	99.8825(15)[q]	97.7(8)[u]	98.0(14)[y]
		101.3240(16)[m]		99.1(20)[v]	
Br	∼112[h]	102.7(3)[k]	101.0(3)[r]	99.7(20)[w]	99.9(10)[z]
		103.1(4)[l]		98.6(7)[u]	
				100.0(20)[v]	
I	-	-	102.1(10)[s]		99.9(12)[t]
				103.5(9)[u]	
				105.3[v]	

[a] The few experimental data of the $^3B_1$ state AX_2 molecules: CH_2 r_o = 1.078 Å and ∠ ∼136° (ref 42) and r_e = 1.0766(14) Å and ∠ = 134.037(45)° (ref 43); SiF_2 r_o = 1.586(1) Å and ∠ =113.1(1)° (ref 44); $SiCl_2$ r_e = 2.041(5) Å and ∠ =114.5 or 115.4 (ref 45). [b] Bond lengths are r_g parameters from ED, unless otherwise indicated. [c] r_e from infrared flash-kinetic spectroscopy, ref 46. [d] r_0 from microwave spectroscopy (MW), ref 47. [e] r_0 from ultraviolet spectroscopy (UV), ref 48. [f] r_0 from MW, ref 49. [g] r_0 from laser induced fluorescence (LIF), refs 50 and 51. [h] r_a from ED, probably in error, ref 52. [i] r_e from infrared spectroscopy (IR), ref 53. [j] r_e from MW refs 54 and 55. [k] Reference 56. [l] r_e from joint ED and vibrational spectroscopic analysis (ED + SP), ref 57. [m] r_e from MW, ref 58. [n] r_0 from LIF, ref 59. [o] r_e from MW, ref 60. [p] Reference 61. [q] r_e from MW, ref 62. [r] References 63 and 64. [s] r_α from ED, ref 65. [t] Reference 66. [u] r_e from ED + SP, ref 67. [v] r_e from ED + SP, ref 68. [w] Reference 69. [x] Reference 70. [y] Reference 71. [z] Reference 72.

and bond angles are given in Table 3. Singlet−triplet separations as obtained from different computations are collected in Table 4.

We tried to assess the effect of the computational level on the structural parameters, and for that reason we compared our results with some earlier results on methylene and halocarbenes; see Table 1S in the Supporting Information.

As for equilibrium geometries, computed parameters undoubtedly superior to our two CCSD(T) series, were only found for CH_2,[34] CCl_2,[10] and CBr_2.[8] Singlet−triplet separations as obtained from a better computation have been published for all CX_2 species. Among the values quoted in Table 1S there are numbers of higher quality and of comparable quality (in some cases it is difficult to determine which description of electron correlation is better) whereas some of the results are of slightly lower quality than our CCSD(T) calculations. From this we can conclude that the change in the quality of the theoretical description at this relatively high level affects the computed numbers only slightly (bond lengths change mostly less than 0.03 Å, bond angles less than 1.5°). Thus, we feel confident that qualitatively correct conclusions can be drawn on the basis of our CCSD(T) calculations.

Ground State. The variation of bond lengths in the $^1A_1$ state of AX_2 molecules down group 14 is given in Figure 1. For all molecules, except for CH_2, this is the ground state of the system.

The general trend in the variation of geometrical parameters is the same from all computations and also from experiment; i.e., the bond lengths increase in going from carbon as the central atom toward lead with the same halogen ligand. The same trend is observed in the series of the same central atom in going from the dihydrides to the diiodides. These trends are what we expect, due to the change in atomic sizes.[16,17]

Comparing the bond lengths from different computations, the actual data tend to scatter more as we go toward the larger halides. Bond lengths from the density functional calculations of Escalante et al.[18] are systematically larger than from all the other methods. The MRSDCI/EC calculation, though in good agreement with our computed values from CX_2 to SnX_2, gives much larger Pb−X bond lengths for all ligands.

Comparison of the calculated and experimental bond lengths is always difficult due to the different physical meaning of these parameters.[35,36] While the computed bond lengths are the equilibrium bond lengths and as such correspond to the minimum of the potential energy surface, the experimental bond lengths are always averaged values, and the averaging depends on the experimental method. Two bond distance types are found most often for AX_2 molecules. One of them is a near-r_e distance from microwave spectroscopy obtained with appropriate procedure. This parameter is ideal to compare with the computations. The thermal average distance, r_g, coming from electron diffraction (ED) studies, on the other hand, is always longer

TABLE 4: Computed Singlet-Triplet Gaps (kcal mol^{-1}) for AX_2 Molecules (A = C, Si, Ge, Sn, Pb; X = H, F, Cl, Br, I)

	C		Si		Ge			Sn			Pb		
	a	*b*	*a*	*b*	*a*	*b*	*c*	*a*	*b*	*c*	*a*	*b*	*c*
F	56.4	56.4	73.5	73.5	82.1	83.3	78.6	75.0	77.1	72.9	91.9	94.9	95.7
Cl	19.8	19.8	53.0	53.0	61.4	62.6	60.3	60.1	61.7	60.0	73.9	75.9	71.0
Br	15.8	16.3	47.7	48.1	55.2	56.2	54.4	54.7	56.4	55.5	65.6	68.0	64.4
I	8.3	9.2	38.9	39.7	45.9	46.6	42.2	46.4	48.0	47.1	55.0	57.5	54.8
H	−10.4	−10.4	20.0	20.0	22.0	25.1	23.2	23.4	25.9	24.5	34.0	35.0	33.1

[a] CCSD(T)/EC. [b] CCSD(T)/ST. [c] MRSDCI/EC; MRSDCI+Q values indicated for GeF_2, SnF_2, and PbF_2. See text and original publications for other details.

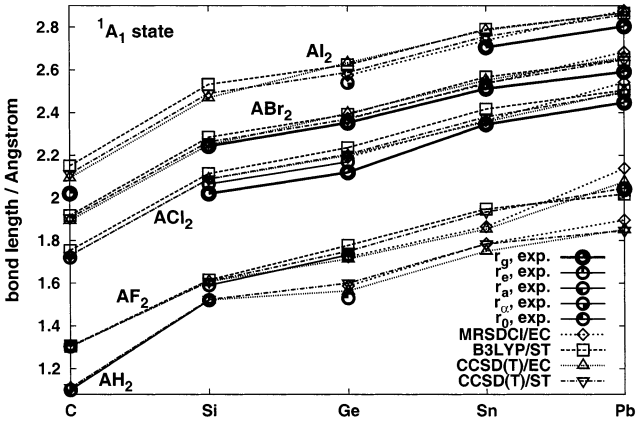

Figure 1. Bond length variation of AX_2 molecules in their $^1A_1$ state. MRSDCI/EC from refs 14−17; B3LYP/ST from ref 18; CCSD(T)/EC and CCSD(T)/ST present work. For more details see text.

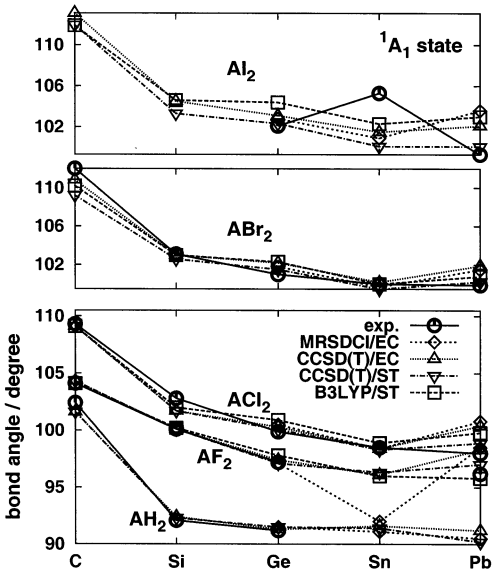

Figure 2. Bond angle variation of AX_2 molecules in their $^1A_1$ state. For abbreviations see caption of Figure 1.

than the r_e parameter. Not to cause any confusion, in our figures only the physically comparable experimental distances are connected with a line.

As Figure 1 indicates, the larger the central atom, and the larger the halogen size, the larger are the differences between computed and experimental bond lengths. The difference is especially conspicuous, as the computed bond lengths appear to be larger than the experimental ones in the heavier molecules, especially in the bromides and iodides. Because the heaviest AX_2 molecules ($GeBr_2$, GeI_2, $SnCl_2$, $SnBr_2$, SnI_2, PbF_2, $PbCl_2$, $PbBr_2$, PbI_2) were studied by gas-phase ED, the computed bond lengths would fall even more off the hypothetical experimental equilibrium distances than from the r_g values indicated in the figures. At the same time, these heavy molecules are the very systems for which the accuracy of the computational technique is most difficult to judge (due to the incompleteness of the basis sets, truncations in the configurations' space, use of ECPs, etc.). Therefore, it is fortunate that in judging the computational results, we can rely on the comparison with the ED bond lengths, which are precisely determined parameters.

Interestingly, the reliability of bond angles is just the opposite. Due to the high temperatures of the electron diffraction experiments and the floppiness of these molecules, the halogen···halogen distances are not well determined from ED, this affects the reliability of the bond angles,[36] as is apparent from Figure 2 for the iodides. Consequently, bond angles tend to be more reliable from the computations than from the experiment. Also, a comparison of bond angles from different sources suffers less from the indeterminacy of the physical meaning of the parameters than in the case of bond lengths. The bond angle is related to the ratio of the two distances; hence some of the systematic errors cancel.

Figure 2 shows the bond angle variation in the singlet state molecules down group 14. The bond angle of all molecules is smaller than 120°, in agreement with the VSEPR model.[37] The repulsion by the lone electron pair on the central atom of these singlet molecules is larger than the repulsion of a bonding pair; therefore, the ideal angle of 120° should decrease. This angle is between 102° and 112° in the CX_2 molecules. In going from C to Sn as the central atom, the bond angles decrease further, again, as can be explained by the VSEPR model. There is, however, an increase of the angle for all PbX_2 molecules. This can be due to relativistic effects, which cause a contraction of the 6s orbital and lead to a bond angle increase, as pointed out earlier.[17,18]

It is also interesting to note that the degree of angle change along the different AX_2 series is very different. When we consider the hydrides, the decrease of the angle is about 10° on going from CH_2 to SiH_2. On the other hand, the same difference when going from CF_2 to SiF_2 is merely 4°. The large electronegativity of F should, in principle, cause a large angle decrease. However, this same large electronegativity gives rise to a stronger Coulombic repulsion between the ligands, acting against the decrease of the angle. On going toward the larger halides and comparing the CX_2/SiX_2 angle changes, they become larger and larger, so eventually for the CI_2/SiI_2 pair, it is almost as much as for the hydrides, about 9°.

$^3B_1$ State. The computed geometrical parameters for the triplet state AX_2 molecules are given in Tables 1 and 2, and the variation of the geometrical parameters is shown in Figures 3 and 4. The qualitative trend in their variation is similar to that of the singlets. However, if we compare the actual geometrical parameters for the singlet and triplet states of the same molecule, we find interesting differences. The most noticeable difference is that the bond angle in the triplets is much larger, by about

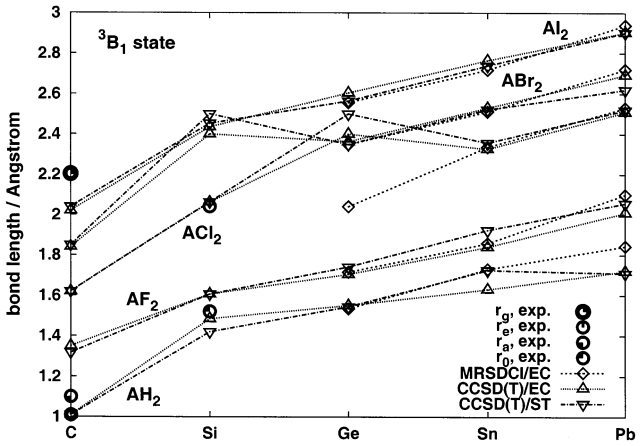

Figure 3. Bond length variation of AX_2 molecules in their $^3B_1$ state. For abbreviations see caption of Figure 1.

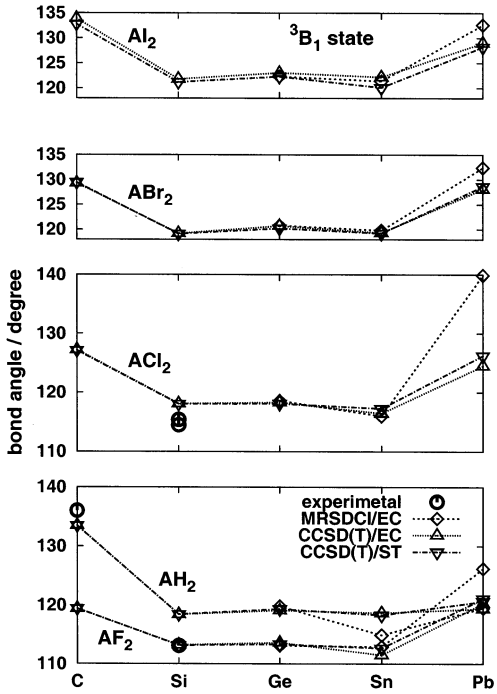

Figure 4. Bond angle variation of AX_2 molecules in their $^3B_1$ state. For abbreviations see caption of Figure 1.

10−30°, than in the singlets for all AX_2 molecules.[6,7,16,17] This can be rationalized with the VSEPR model.

In the singlet state, the HOMO is of a_1 symmetry, which qualitatively corresponds to the lone pair of electrons lying in the molecular plane. The lone pair, exercising a large space requirement, results in a bond angle smaller than 120°. In the triplet state one of these electrons is moved to an orbital of b_1 symmetry, which is essentially the out-of-plane atomic p orbital of the central atom. Thus, regarding the valence shell electrons in the molecular plane, there is only one electron left on the central atom, and this leads to a decreased repulsion and a consequent opening of the bond angle as compared to the singlet state (see also ref 38).

The other notable difference between the singlet and triplet geometries, shown by computations as well as by experiments, where available, is that bonds are in most cases shorter in the triplets than in the singlets. This is just the opposite of what one would expect, regarding that in all cases, except for CH_2, the $^3B_1$ state is the first excited state of the system. To analyze this phenomenon somewhat more in detail, Mayer's chemical

TABLE 5: Diatomic Contributions of the SCF Energy (au) for the Ground State and First Excited State of CX_2 Molecules (X = H, F, Cl, Br), As Obtained from the CECA Analysis of Mayer (Ref 39)[a]

	C−X	X···X
CH_2		
$^1A_1$	−0.4891	0.0290
$^3B_1$	−0.5025	0.0257
CF_2		
$^1A_1$	−0.5604	0.0732
$^3B_1$	−0.5234	0.0487
CCl_2		
$^1A_1$	−0.3481	0.0523
$^3B_1$	−0.3489	0.0358
CBr_2		
$^1A_1$	−0.3687	0.0537
$^3B_1$	−0.3860	0.0448

[a] 6-311G basis set, geometries are optimized at the SCF level.

energy component analysis[39,40] was carried out for the RHF/UHF wavefunction of the singlet/triplet states of CX_2 molecules, using the 6-311G basis set at the HF optimized geometry. The diatomic contributions of the SCF energies, collected in Table 5, underline the trends shown by the geometries: the repulsive interaction between the ligands decreases on going from the singlets to the triplets. At the same time the C−X component, measuring the interaction between the central atom and the ligand, gets larger in all cases where the bond gets shorter. The origin of this effect may again lie in the decreasing electron density around the central atom in the molecular plane, as we go from the singlet to the triplet state. Thus, the ligands can get closer to the central atom and achieve a better screening of the bonding electrons. The opening of the bond angle could in principle also explain the shortening of the bond, however, reoptimizing the bond lengths of the triplets at the bond angles of the singlets, gave less than 50% of the effect.

The bond angle of all triplet PbX_2 molecules is much larger than those of the SnX_2 molecules. This effect in the triplets is much more pronounced than in the singlets.

Comparing the triplet bond angles from different calculations, the agreement is acceptable. The MRSDCI method gives a much larger X−Pb−X angle[17] than the CCSD(T) method for all halides. Comparison with experimental bond angles is not possible because there are only a few experimental geometries available for the triplets.

Effect of Quasi-Relativistic Treatment. We address two issues in this section, both related to the quasi-relativistic description of the inner shell electrons of the atoms. One of them is whether any break or other artificial effect is introduced in the trends showing the variation of the geometrical parameters at the point where we substitute the atomic cores by an effective potential. This question arises as the application of an effective potential introduces one more approximation into the theoretical description.

The other point is connected to the advantage of the application of ECPs, i.e., the possibility to switch scalar relativistic effects on and off. Here we study the effect of relativity on the geometry of molecules containing atoms of large atomic number.

To characterize the change that the introduction of an ECP induces, two series of equilibrium parameters were computed. In these calculations we altered the quasi-relativistic and nonrelativistic description of the cores at a stage where relativistic effects are expected to be yet unimportant. The results are reported in Table 6, the first lines corresponding to the application of quasi-relativistic ECPs only from the fifth row

TABLE 6: Comparison of Computed Equilibrium Parameters of AX_2 Molecules with Different Approximations[a]

elec state	$^1A_1$					$^3B_1$				
	C	Si	Ge	Sn	Pb	C	Si	Ge	Sn	Pb
					r_e(A−X)/Å					
H		1.523	1.597				1.484	1.545		
		1.515	1.600				1.474	1.544		
F		1.608	1.781				1.606	1.773		
		1.607	1.750				1.603	1.741		
Cl	1.730	2.089	2.193	2.380	2.494	1.685	2.063	2.166	2.357	2.519
	1.718	2.078	2.188	2.363	2.483	1.675	2.049	2.160	2.340	2.505
Br	1.892	2.262	2.357	2.543	2.650	1.833	2.229	2.329	2.522	2.686
	1.906	2.268	2.370	2.539	2.648	1.850	2.240	2.349	2.522	2.687
I		2.490	2.574				2.453	2.544		
		2.499	2.588				2.460	2.564		
					∠(X−A−X)/deg					
H		92.3	91.8				118.4	119.4		
		91.5	91.2				117.9	119.3		
F		100.7	96.5				113.2	111.3		
		100.0	97.8				113.7	113.3		
Cl	109.1	101.6	100.2	98.4	98.9	127.8	118.1	118.0	117.3	126.3
	109.5	101.4	100.0	97.5	98.6	127.6	119.1	118.3	115.9	124.7
Br	109.9	102.2	101.2	99.0	99.7	129.5	119.6	119.7	118.7	127.4
	109.9	102.2	101.5	99.5	100.3	129.4	120.0	120.85	119.2	128.6
I		103.3	102.4				121.2	121.4		
		103.1	102.4				121.0	122.3		

[a] CCSD(T) within the frozen core approximation. First lines: quasi-relativistic ECPs of the Stuttgart/Bonn group on atoms Sn, I, and Pb. Second lines: quasi-relativistic ECPs of the Stuttgart/Bonn group on atoms Si, Cl, Ge, Br, Sn, I, and Pb. See text for other details.

TABLE 7: Computed Equilibrium Bond Lengths (Å) and Bond Angles (deg) of the $^1A_1$ and $^3B_1$ State of PbX_2 Molecules (X = H, F, Cl, Br, I), Applying Quasi-Relativistic (QR) and Nonrelativistic (NR) Core on Atoms Br, I, and Pb[a]

	$^1A_1$				$^3B_1$			
	r_e(A−X)		∠(X−A−X)		r_e(A−X)		∠(X−A−X)	
	NR	QR	NR	QR	NR	QR	NR	QR
H	1.866	1.847	91.6	90.9	1.811	1.773	117.7	120.6
F	2.007	2.045	94.8	97.1	2.001	2.056	111.5	121.5
Cl	2.473	2.493	96.1	98.9	2.449	2.519	115.4	126.3
Br	2.639	2.648	96.9	100.3	2.615	2.687	116.5	128.6
I	2.842	2.858	98.4	100.8	2.816	2.902	118.0	128.2

[a] CCST(T) with frozen core on atoms Br, I, and nonrelatvistic ECP on Pb in the case of NR. Relativistic ECPs of the Stuttgart/Bonn group were used for atoms Br, I, and Pb in the case of QR. For other details see text.

on, whereas values of the second lines are results from using ECPs starting from the third row of the periodic table. The two series lie fairly close to each other. The bond length changes typically remain under 0.02 Å, whereas the bond angles are mostly affected by less than 2°.

In the case of atoms of large atomic numbers, like Pb or I, it is interesting to check whether any effect of relativity appears on the geometry. As to the bond lengths, a relativistic contraction can be expected to occur for the heavier lead halides, but this is not observed. Interestingly, it is the bond angles that show the signs of relativistic effects, in that they increase rather than decrease in all lead halides compared with the tin halides. To see whether this increase of the bond angle in lead dihalides can be attributed to relativistic effects, equilibrium geometries, obtained by applying a quasi-relativistic description of the core electrons, are compared to nonrelativistic results in Table 7. From the table it is apparent that the bond angle opens upon switching on the quasi-relativistic treatment. This is interesting, because it had been suggested that the relativistic effect on bond angles should be slight.[41] Of course, the present case does not make it possible to distinguish between the basis set and relativistic effects, so it is hard to draw a definite conclusion on relativistic effects on the basis of these numbers. At the same time, experience with group 15 trihalides, from both experiment and computation, shows the same effect in the BiX_3 trihalides as we observe here for the PbX_2 dihalides.[36]

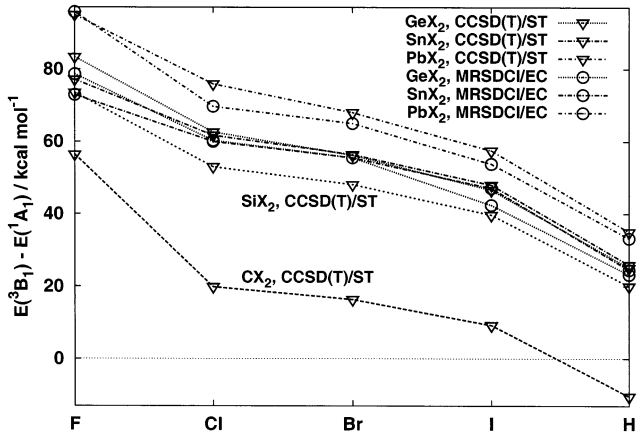

Figure 5. Singet−triplet separation of AX_2 molecules. For abbreviations see text. For fluorides MRSDCI+Q is plotted from ref 15.

Singlet−Triplet Energy Gaps. Table 4 gives the singlet−triplet energy separations for all molecules, and their variation is shown in Figure 5. The trend is apparent; the largest separation appears in the fluorides for all central atoms and it decreases toward the iodides as observed earlier, see, e.g., refs 6, 7, 11, 16, and 17. Hydrogen occupies a position after iodine; that is, the separation is the smallest for the hydrides.

Considering a molecular orbital (MO) picture, it is two orbitals in carbene and all its analogues whose occupancy determines whether we have a singlet, $^1A_1$, state or a triplet, $^3B_1$, state. In the singlet state the a_1-symmetry molecular orbital is the HOMO. This is a σ-type antibonding orbital having contributions from the in-plane p orbitals of the central atom and from the in-plane p orbitals of the substituents in opposite phase. Taking the CX_2 series, for example, and inspecting the effect of electronegativity and size of the substituent on the HOMO, we can see the following. In the case of a highly electronegative ligand, like fluorine, the contribution of the

carbon s orbital to the bonding will be large, decreasing the energy of the a_1 orbital. This leads to an increase of the HOMO−LUMO gap, favoring electron pairing, i.e., the singlet state.

If we look at the b_1 orbital, it is the LUMO in the singlet states but becomes the HOMO for the triplets as one of the electrons from the singlet a_1 orbital moves to this b_1 orbital. This is a p-type antibonding orbital, consisting of the carbon out-of-plane p orbital and the out-of-plane p orbitals of the ligands in opposite phase. For the same very electronegative ligand, fluorine, this will be a strongly antibonding orbital, therefore, its energy will be high. That means that the gap between the a_1 and b_1 orbitals will be large.

With decreasing electronegativity of the ligand, the contribution of the carbon s orbitals to the a_1 MO decreases, raising the energy of this orbital. At the same time, for the triplet states, with decreasing electronegativity and increasing size of the ligands, the energy of their out-of-plane p orbital increases. Therefore, the overlap of these orbitals with the carbon p orbital decreases, and so does the antibonding nature of the b_1 orbital, lowering the energy of that orbital. Thus, in going from the fluorides toward the iodides, the a_1 and b_1 orbitals get closer and closer to each other, and their energy separation decreases. Hydrogen comes after iodine in this series, and for CH_2 alone in the series, the triplet becomes the ground state.

IV. Conclusion

The geometrical parameters of the dihydrides and dihalides of all group 14 elements have been calculated at the CCSD(T) level for both their ground state and first excited state. The ground state for all molecules, except CH_2, is of $^1A_1$, whereas their first excited state is of $^3B_1$ symmetry. The singlet−triplet energy separations have also been calculated.

The variation of the geometrical parameters of the singlets follows the expected trend both along the series of group 14 atoms with the same ligand and according to the increasing size of the ligands for the same central atom. The bond angles of the PbX_2 molecules appear to be larger for all ligands than those of the SnX_2 molecules, in contrast to the trend followed by all other molecules. This can be explained by the influence of relativistic effects on the heavy lead atom and our test calculations with nonrelativistic ECPs confirmed this. In this regard it is surprising that this effect does not show up in the bond lengths of the lead dihalides. The trends observed in the triplet series are similar to those for the singlets, with the relativistic increase for lead dihalides appearing even more strongly here.

The bonds of the triplets are in most cases shorter than those of the singlets, and this is surprising, considering that the singlets are the ground state for all molecules except CH_2. There is, at the same time, a substantial increase, by 10−30°, in the bond angles of the triplets compared with those of the singlets. These changes may be explained by the decreasing electron density in the molecular plane of the triplets due to an electron moving from the a_1 symmetry in-plane MO to the b_1 symmetry out-of-plane MO compared with the singlets.

Comparison of computed and experimental geometries is the best way to assess the reliability of the computations. In this respect the bond lengths and the bond angles have to be looked at somewhat differently. The bond lengths from experiment are precise and so they are good tests for the computation, provided that the differences in their physical meaning is taken into account. Although the agreement is good for the lighter molecules, it worsens as the size of the molecules increases, with the computed bond lengths appearing too long. As to the bond angles, they are more reliable from the computation than from electron diffraction experiments, where they suffer from the high experimental temperatures and the floppiness of these molecules.

Comparing the performance of different theoretical methods and basis sets on the computed geometries, the following conclusions can be drawn. Density functional B3LYP results fall somewhat off from other methods and from experiment, but without affecting the qualitative trend shown by the numbers. Among the computations presented, it is CCSD(T) used with the effective core potential of the Stuttgart/Bonn group that gives equilibrium bond lengths running almost parallel with the experimental curves and lying the closest to it at the same time. The bond angle opening of lead dihalides as compared to the tin analogues is the largest when applying the effective core potentials of Christiansen et al., irrespective of the theoretical method (MRSDCI or CCSD(T)).

Inclusion of the $(n - 1)$d shell of the central atom in the valence space was not found necessary. Rather, unbalanced data sets of equilibrium geometries were obtained when a smaller effective core of Christiansen et al. was used together with a larger valence basis. Apart from the carbon derivatives, among the computed equilibrium geometries available to date, the present CCSD(T)/ST geometries are of the highest computational level, to our knowledge.

Acknowledgment. We thank Professor Péter R. Surján for his helpful comments and suggestions. Calculations were performed on the four Compaq AlphaServer 4100 machines of the Eötvös University, Budapest. Financial support of the Hungarian Scientific Research Fund (Grant No. OTKA T037978) is gratefully acknowledged.

Supporting Information Available: Comparison of equilibrium bond lengths, bond angles, and singlet−triplet gaps for CX_2 molecules computed at different levels of theory. This material is available free of charge via the Internet at http://pubs.acs.org.

Note Added after ASAP Posting. This article was released ASAP on 5/3/2003. In Table 3, column 3, row 6, 2.706(4) was changed to 2.076(4), and in column 5, row 11, 2.076(4) was changed to 2.706(4). The correct version was posted on 5/13/2003.

References and Notes

(1) Hargittai, M.; Schultz, G.; Hargittai, I. *Russ. Chem. Bull*. **2001**, *50*, 1.
(2) Yamaguchi, Y.; Sherrill, C. D.; Schaefer, H. F. *J. Phys. Chem.* **1996**, *100*, 7911.
(3) Sherrill, C. D.; Huis, T. J. V.; Yamaguchi, Y.; Schaefer, H. F. *J. Mol. Struct. (THEOCHEM)* **1997**, *400*, 139.
(4) Sherrill, C. D.; Leininger, M. L.; Huis, T. J. V.; Schaefer, H. F. *J. Chem. Phys*. **1998**, *108*, 1040.
(5) Garcıa, V. M.; Castell, O.; Reguero, M.; Caballol, R. *Mol. Phys*. **1996**, *87*, 1395.
(6) Das, D.; Whittenburg, S. L. *J. Mol. Struct. (THEOCHEM)* **1999**, *492*, 175.
(7) Schwartz, M.; Marshall, P. *J. Phys. Chem*. **1999**, *A 103*, 7900.
(8) Sendt, K.; Bacskay, G. B. *J. Chem. Phys*. **2000**, *112*, 2227.
(9) Schwartz, R. L.; Davico, G. E.; Ramond, T. M.; Lineberger, W. C. *J. Phys. Chem*. **1999**, *A 103*, 8213.
(10) Barden, C. J.; Schaefer, H. F. *J. Chem. Phys*. **2000**, *112*, 6515.
(11) Lee, E. P. F.; Dyke, J. M.; Wright, T. G. *Chem. Phys. Lett*. **2000**, *326*, 143.
(12) Hajgató, B.; Nguyen, H. M. T.; Veszprémi, T.; Nguyen, M. T. *Phys. Chem. Chem. Phys*. **2000**, *2*, 5041.
(13) Hargittai, M.; Schultz, G.; Schwerdtfeger, P.; Seth, M. *Struct. Chem.* **2001**, *12*, 377.

(14) Balasubramanian, K. *J. Chem. Phys.* **1988**, *89*, 5731.
(15) Dai, D.; Al-Zahrani, M. M.; Balasubramanian, K. *J. Phys. Chem.* **1994**, *98*, 9233.
(16) Benavides-Garcıa, M.; Balasubramanian, K. *J. Chem. Phys*. **1992**, *97*, 7537.
(17) Benavides-Garcıa, M.; Balasubramanian, K. *J. Chem. Phys*. **1994**, *100*, 2821.
(18) Escalante, S.; Vargas, R.; Vela, A. *J. Phys. Chem*. **1999**, *A 103*, 5590.
(19) Pacios, L.; Christiansen, P. *J. Chem. Phys*. **1985**, *82*, 2664.
(20) Hurley, M.; Pacios, L.; Christiansen, P.; Ross, R.; Ermler, W. *J. Chem. Phys*. **1986**, *84*, 6840.
(21) LaJohn, L.; Christiansen, P.; Ross, R.; Atashroo, T.; Ermler, W. *J. Chem. Phys*. **1987**, *87*, 2812.
(22) Ross, R.; Powers, J.; Atashroo, T.; Ermler, W.; LaJohn, L.; Christiansen, P. *J. Chem. Phys*. **1990**, *93*, 6654.
(23) Bergner, A.; Dolg, M.; Küchle, W.; Stoll, H.; Preuss, H. *Mol. Phys*. **1993**, *80*, 1431.
(24) Frisch, M. J.; Trucks, G. W.; Schlegel, H. B.; Scuseria, G. E.; Robb, M. A.; Cheeseman, J. R.; Zakrzewski, V. G.; Montgomery, J. A., Jr.; Stratmann, R. E.; Burant, J. C.; Dapprich, S.; Millam, J. M.; Daniels, A. D.; Kudin, K. N.; Strain, M. C.; Farkas, O.; Tomasi, J.; Barone, V.; Cossi, M.; Cammi, R.; Mennucci, B.; Pomelli, C.; Adamo, C.; Clifford, S.; Ochterski, J.; Petersson, G. A.; Ayala, P. Y.; Cui, Q.; Morokuma, K.; Malick, D. K.; Rabuck, A. D.; Raghavachari, K.; Foresman, J. B.; Cioslowski, J.; Ortiz, J. V.; Stefanov, B. B.; Liu, G.; Liashenko, A.; Piskorz, P.; Komaromi, I.; Gomperts, R.; Martin, R. L.; Fox, D. J.; Keith, T.; Al-Laham, M. A.; Peng, C. Y.; Nanayakkara, A.; Gonzalez, C.; Challacombe, M.; Gill, P. M. W.; Johnson, B. G.; Chen, W.; Wong, M. W.; Andres, J. L.; Head-Gordon, M.; Replogle, E. S.; Pople, J. A. *Gaussian 98*, revision A.7; Gaussian, Inc.: Pittsburgh, PA, 1998.
(25) Binning, R.; Curtiss, L. *J. Comput. Chem*. **1990**, *11*, 1206.
(26) Glukhovtsev, M.; Pross, A.; McGrath, M.; Radom, L. *J. Chem. Phys*. **1995**, *103*, 1878.
(27) Dunning, T. J., Jr. *Chem. Phys*. **1989**, *90*, 1007.
(28) Woon, D.; Dunning, T. J., Jr. *Chem. Phys*. **1993**, *98*, 1358.
(29) http://www.theochem.uni-stuttgart.de/.
(30) Martin, J.; Sundermann, A. J. *Chem. Phys*. **2001**, *114*, 3408.
(31) Küchle, W.; Dolg, M.; Stoll, H.; Preuss, H. *Mol. Phys*. **1991**, *74*, 1245.
(32) Extensible Computational Chemistry Environment Basis Set Database, Version 4/05/02, as developed and distributed by the Molecular-Science Computing Facility, Environmental and Molecular Sciences Laboratory which is part of the Pacific Northwest Laboratory, P.O. Box 999, Richland, WA 99352, and funded by the U.S. Department of Energy. The Pacific Northwest Laboratory is a multiprogram laboratory operated by Battelle Memorial Institue for the U.S. Department of Energy under contract DE-AC06-76RLO 1830. Contact David Feller or Karen Schuchardt for further information or visit http://www.emsl.pnl.gov:2080/docs/home-page.html.
(33) Wilson, A.; Woon, D.; Peterson, K.; Dunning, T. J., Jr. *Chem. Phys*. **1999**, *110*, 7667.
(34) Woon, D. E.; Dunning, T. H., Jr. *J. Chem. Phys*. **1995**, *103*, 4572.
(35) Hargittai, M.; Hargittai, I. *Int. J. Quantum Chem*. **1992**, *44*, 1057.
(36) Hargittai, M. *Chem. Rev*. **2000**, *100*, 2233.
(37) Gillespie, R.; Hargittai, I. *The VSEPR Model of Molecular Geometry*; Allyn and Bacon: Boston, 1991.
(38) Liebman, J.; Simons, J. In *Molecular Structure and Energetics*; Liebman, J.; Greenberg, A., Eds.; VCH Publishers: New York, 1986; Vol. 1; pp. 51−99.
(39) Mayer, I. *Chem. Phys. Lett*. **2000**, *332*, 381.
(40) Program APOST, Version 1.0, Budapest, April 2000 (Available via the Internet at the address http://occam.chemres.hu/programs or by anonymous ftp at the address (ftp://)kvk.chemres.hu).
(41) Pyykkö, P. *Chem. Rev*. **1988**, *88*, 563.
(42) Herzberg, G.; Johns, J. W. C. *J. Chem. Phys*. **1971**, *54*, 2276.
(43) Bunker, P. R.; Jensen, P.; Kraemer, W. P.; Beardsworth, R. J. *Chem. Phys*. **1986**, *85*, 3724.
(44) Karolczak, J.; Judge, R. H.; Clouthier, D. J. *J. Am. Chem. Soc*. **1995**, *117*, 952.
(45) Chau, F.-T.; Wang, D.-C.; Lee, E. P. F.; Dyke, J. M.; Mok, D. K. W. *J. Phys. Chem*. **1999**, *A 103*, 4925.
(46) Petek, H.; Nesbitt, D. J.; Darwin, D. C.; Ogilby, P. R.; Moore, C. B.; Ramsay, D. A. *J. Chem. Phys*. **1989**, *91*, 6566.
(47) Kirchhoff, W. H., Jr., D. R. L.; Powell, F. X. *J. Mol. Spectrosc*. **1973**, *47*, 491.
(48) Mathews, C. W. *Can. J. Phys.* **1967**, *45*, 2355.
(49) Fujitake, M.; Hirota, E. *J. Chem. Phys*. **1989**, *91*, 3426.
(50) Clouthier, D. J.; Karolczak, *J. Phys. Chem.* **1989**, *93*, 7542.
(51) Clouthier, D. J.; Karolczak, J. *J. Chem. Phys.* **1991**, *94*, 1.
(52) Ivey, R. C.; Schulze, P. D.; Leggett, T. L.; Kohl, D. A. *J. Chem. Phys*. **1974**, *60*, 3174.
(53) Yamada, C.; Kanamori, H.; Hirota, E.; Nishiwaki, N.; Itabashi, N.; Kato, K.; Goto, T. *J. Chem. Phys*. **1989**, *91*, 4582.
(54) Shoji, H.; Tanaka, T.; Hirota, E. *J. Mol. Spectrosc*. **1973**, *47*, 268.
(55) Rao, V. M.; Curl, R. F.; Timms, P. L.; Margrave, J. L. *J. Chem. Phys*. **1965**, *43*, 2557.
(56) Hargittai, I.; Schultz, G.; Tremmel, J.; Kagramanov, N. D.; Maltsev, A. K.; Nefedov, O. M. *J. Am. Chem. Soc*. **1983**, *105*, 2895.
(57) Gershikov, A. G.; Subbotina, N. Y.; Hargittai, M. *J. Mol. Spectrosc.* **1990**, *143*, 293.
(58) Fujitake, M.; Hirota, E. *Spectrochimica Acta* **1994**, *50A*, 1345.
(59) Karolczak, J.; Harper, W. W.; Grev, R. S.; Clouthier, D. J. *J. Chem. Phys*. **1995**, *103*, 2839.
(60) Takeo, H.; R. F. C., Jr. *J. Mol. Spectrosc*. **1972**, *43*, 21.
(61) Schultz, G.; Tremmel, J.; Hargittai, I.; Berecz, I.; Bohátka, S.; Kagramanov, N. D.; Maltsev, A. K.; Nefedov, O. M. *J. Mol. Struct*. **1979**, *55*, 207.
(62) Tsuchiya, M. J.; Honjou, H.; Tanaka, K.; Tanaka, T. *J. Mol. Struct*. **1995**, 352/353, 407.
(63) Schultz, G.; Tremmel, J.; Hargittai, I.; Kagramanov, N. D.; Maltsev, A. K.; Nefedov, O. M. *J. Mol. Struct*. **1982**, *82*, 107.
(64) Schultz, G.; Kolonits, M.; Hargittai, M. *Struct. Chem*. **2000**, *11*, 161.
(65) Giricheva, N. I.; Girichev, G. V.; Shlykov, S. A.; Titov, V. A.; Chusova, T. P. *J. Mol. Struct*. **1995**, *344*, 127.
(66) Gershikov, A. G.; Zasorin, E. Z.; Demidov, A. V.; Spiridonov, V. P. *Zh. Strukt. Khim*. **1986**, *27*, 36.
(67) Nasarenko, A. Y.; Spiridonov, V. P.; Butayev, B. S.; Zasorin, E. Z. *J. Mol. Struct. (THEOCHEM)* **1985**, *119*, 263.
(68) Ermakov, K. V.; Butayev, B. S.; Spiridonov, V. P. *J. Mol. Struct*. **1991**, *248*, 143.
(69) Demidov, A. V.; Gershikov, A. G.; Zasorin, E. Z.; Spiridonov, V. P. *Zh. Strukt. Khim*. **1983**, *24*, 9.
(70) Bazhanov, V. I. *Zh. Strukt. Khim*. **1991**, *32*, 54.
(71) Hargittai, I.; Tremmel, J.; Vajda, E.; Ishchenko, A. A.; Ivanov, A. A.; Ivashkevich, L. S.; Spiridonov, V. P. *J. Mol. Struct*. **1977**, *42*, 147.
(72) Ishchenko, A. A.; Tarasenko, Y. I.; Spiridonov, V. P. *Struct. Chem.* **1990**, *1*, 217.